Evolutionary diversification of alpine ginger reflects the early uplift of the Himalayan–Tibetan Plateau and rapid extrusion of Indochina

Jian-Li Zhao [a,1], Yong-Mei Xia [a,1], Charles H. Cannon [a,b], W. John Kress [a,c], Qing-Jun Li [a,*]

[a] Key Laboratory of Tropical Forest Ecology, Xishuangbanna Tropical Botanical Garden, Chinese Academy of Sciences, Mengla, Yunnan 666303, PR China
[b] Department of Biological Sciences, Texas Tech University, Box 43131, Flint and Main Street, Lubbock, TX 79409-3131, USA
[c] Department of Botany, MRC-166, National Museum of Natural History, P.O. Box 7012, Smithsonian Institution, Washington, DC 20013-7012, USA

ABSTRACT

The evolutionary diversifications of many taxonomic groups, especially those with limited dispersal ability, are often driven by key geological events, such as tectonic drift, continental collisions, and uplifts of mountains. Here, we use full range geographic sampling to create a dated molecular phylogeny for two genera of alpine gingers (Cautleya and Roscoea) in the Pan-Himalaya, and test the correlations between evolutionary diversification of this group and major geological events in the studied region. Our results revealed that the origination of their common ancestor and evolutionary split between the two genera occurred during the middle Eocene and the late Eocene to the early Oligocene, corresponding well to the proposed two early uplifts of the Himalayan–Tibetan Plateau. Roscoea species, the highest elevation gingers known, were then divided into distinct Himalayan and Indochinese clades, simultaneous with the rapid extrusion of Indochina and accompanied by the third Himalayan uplift around the Oligocene/Miocene boundary. This study highlights the importance of evolutionary diversification of plants as an independent line of evidence to reflect tectonic events in the Himalayan–Indochinese region.

1. Introduction

The collision of India with Eurasia, beginning in the early Cenozoic time is the most important geological event in Asia (Yin and Harrison, 2000; Jain, 2014). This long-lasting and still ongoing tectonic process has triggered obvious geological events in the Pan-Himalaya, including the early uplifts of the Himalayan–Tibetan Plateau during the middle Eocene (~40–50 Ma), the Oligocene (~30–40 Ma) (Harrison et al., 1992; Raymo and Ruddiman, 1992; Chung et al., 1998; Tapponnier et al., 2001; Replumaz and Tapponnier, 2003; Aikman et al., 2008), and the Oligocene/Miocene boundary (~22–25 Ma) (Tapponnier et al., 1990; Leloup et al., 2001; Guo et al., 2002; Cao et al., 2011; Liu et al., 2012a) possibly with the further extrusion of Indochina (Yang and Liu, 2009; Che et al., 2010) and the later uplifts from the Miocene to the Pliocene (~15 Ma, ~9–7 Ma and ~5–3 Ma) (Harrison et al., 1992; Shi et al., 1998; An et al., 2001; Spicer et al., 2003). The later large-scale uplifts were believed to have driven evolutionary diversifications of numerous plant and animal groups on/around the Himalayan–Tibetan

Plateau (e.g., Rüber et al., 2004; Liu et al., 2006; Zhang et al., 2006; Wang et al., 2009; see also Favre et al., 2014; Liu et al., 2014). However, up to now, no evidence indicated that the early uplifts and rapid extrusion had driven the continuous diversification of a single plant group (but see Che et al., 2010 for animals), which in turn reflects the successive occurrence of these geological events.

The Ginger Family (Zingiberaceae), a Gondwanan monocot lineage, originated around 105 Ma in the middle Cretaceous, and experienced a major radiation in the late Cretaceous (Kress and Specht, 2005). More than 95% of the species in this family are confined to the lowland tropics (Kress et al., 2002), but two genera (Fig. 1), Cautleya (~2 species) and Roscoea (~21 species), are found at high elevations in the Pan-Himalaya (Cowley, 2007; Auvray and Newman, 2010). Their sister lineage, the genus Hedychium (Kress et al., 2002), is distributed at lower elevations in tropical and subtropical Asia, including the Himalayas (HIM) and the Northern Indochina (NIC). Distribution pattern among these three genera was proposed to be caused by the Himalayan–Tibetan orogeny (Wu, 1994).

The two high-elevation genera are of different species richness and geographic distribution. Cautleya, comprising only two species, is continuously distributed across HIM and NIC (Auvray and Newman, 2010); whereas the species-rich Roscoea forms two disjunct groups in HIM and NIC, respectively, and they were separated by a ~500-kilometer gap (Fig. 1) (Ngamriabsakul et al., 2000;

* Corresponding author at: Xishuangbanna Tropical Botanical Garden, Chinese Academy of Sciences, Yunnan 666303, PR China. Tel.: +86 691 8715471; fax: +86 691 8715070.
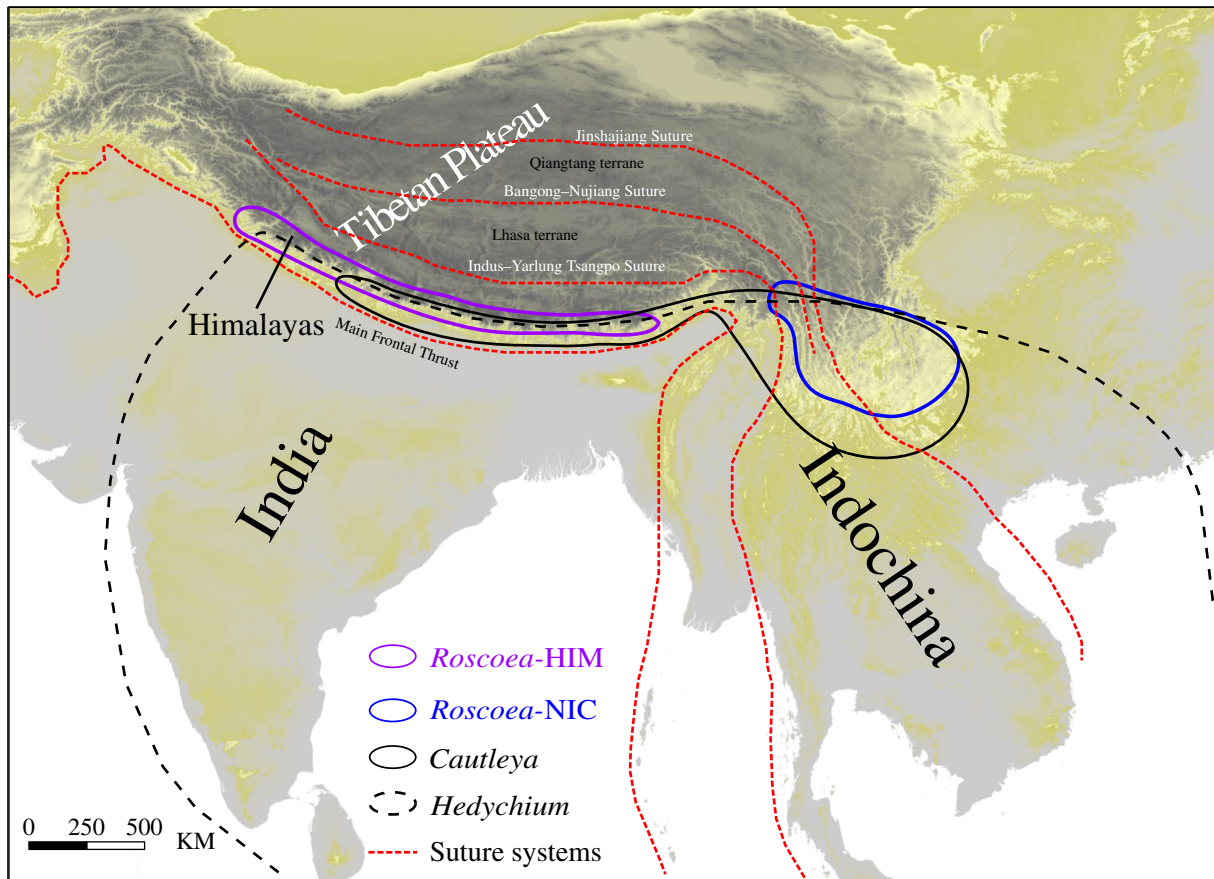E-mail address: qjli@xtbg.ac.cn (Q.-J. Li).
[1] J.L.Z. and Y.M.X. contributed equally to this work.

Fig. 1. Ranges of alpine gingers (*Cautleya* and *Roscoea*) and related genus *Hedychium*. Species of *Cautleya* (black solid) are continuously distributed from the Himalayas (HIM) to the Northern Indochina (NIC), but two species groups of *Roscoea* are disjunct in distribution between HIM (purple solid) and NIC (blue border) by a ~500-kilometer gap. Range of *Hedychium* (black dash) covers Asian subtropics and tropics. Ranges are depicted according to field investigation and references (Wu, 1994; Cowley, 2007; Auvray and Newman, 2010). Sutures systems (red dash) referred to tectonic studies (Yin and Harrison, 2000; Tapponnier et al., 2001; Replumaz and Tapponnier, 2003; Yin, 2010; Chatterjee et al., 2013; Zheng et al., 2013).

Cowley, 2007). These distributional differences between the genera are due, in part, to their distinctive biologies. The species of *Cautleya* (Fig. 2) are terrestrial/epiphytic, insect-pollinated perennials that produce a brightly-colored red capsule with black seeds dispersed by birds (observed in field), and they do not form rhizomatous tubers. In contrast, species of *Roscoea* (Fig. 2) are completely terrestrial, mostly self-pollinated (Zhang and Li, 2008; Fan and Li, 2012)

and possess ant-dispersed seeds, and rhizomatous tubers, which facilitated their frequently vegetative reproduction (Cowley, 2007). These characteristics suggest that long-distance seed dispersal by birds in *Cautleya* is common while seed dispersal capacity is limited in *Roscoea*. The latter genus was likely split into subdivisions by a sudden plate movement due to its poor dispersal ability. Thus, we propose that the contrasting distribution patterns in *Cautleya* and
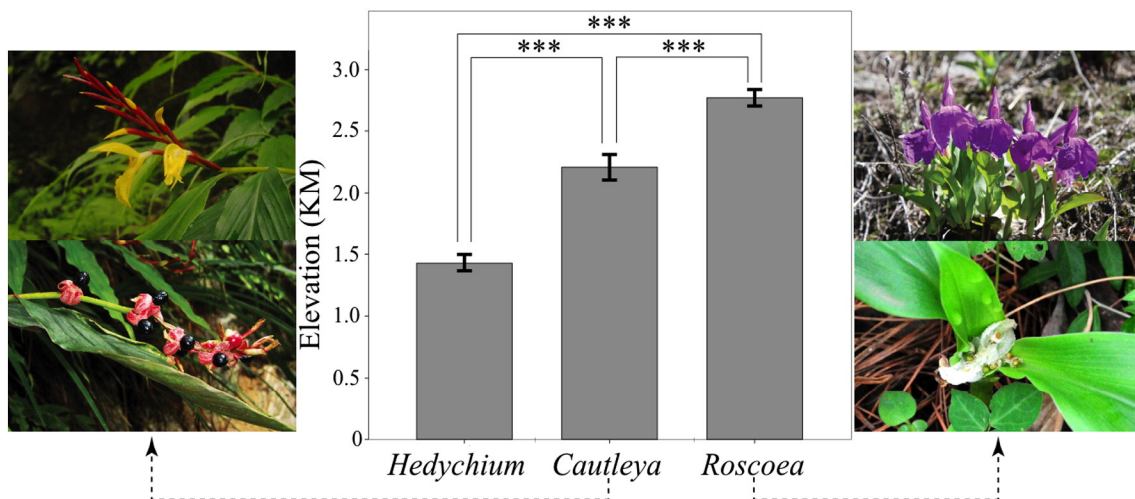
Fig. 2. Elevation differentiation among *Hedychium*, *Cautleya* and *Roscoea*. N is sample size. "***" indicates significant differences between genera ($P < 0.001$). Dashed-line arrows point to the flowers and fruits/seeds of *Cautleya* and *Roscoea*. Sampling sizes for elevation analysis are *Hedychium*: N = 493, *Cautleya*: N = 105 and *Roscoea*: N = 335. Elevation statistics are in Table S1.

Roscoea have been affected not only by the geological history of the region, but also the differences in their morphology and life history, especially the dispersal ability of seeds. Furthermore, we hypothesize that within the genus *Roscoea*, the separation between the HIM and NIC species can be attributed to the vicariant evolution caused by the early uplift of the Himalayan–Tibetan Plateau as well as the rapid lateral extrusion of Indochina at the same time.

In this study, we aimed to use *Cautleya*, *Roscoea* and their close relatives as a model system to test two hypotheses: (*i*) the origination of the common ancestor of *Cautleya* and *Roscoea*, and their subsequent separation, correlated with the two early uplifts of the Himalayan–Tibetan Plateau; and, (*ii*) the split of HIM and NIC species in *Roscoea* is linked to the rapid lateral extrusion of Indochina, synchronous with the third uplift of the Himalayan–Tibetan Plateau.

2. Geological setting

This study focused on the Himalayan–Tibetan orogen and adjacent regions. The Himalayan–Tibetan orogen was shaped by a series of tectonic accretion events since the early Cenozoic. Three main sutures on the Himalayan–Tibetan Plateau are the Jinshajiang Suture, the Bangong–Nujiang Suture and the Indus–Yarlung Tsangpo Suture (Fig. 1), representing the Tethyan relics related to the Indo-Eurasian collision from the Paleogene to the Neogene. These sutures delineate three terranes acting with the Main Frontal Thrust at north and east of India. From north to south, these terranes are the Qiangtang, Lhasa and Himalayas (Yin and Harrison, 2000; Yin, 2006, 2010; Zhang et al., 2012; Chatterjee et al., 2013). The uplifts of the Himalayan–Tibetan Plateau, along with the 90° clockwise rotation at the eastern extension of these sutures and terranes, and the lateral extrusion of Indochina, are all outcomes of the cumulative Cenozoic deformation of SE Asia as caused by underthrusting of the Indian Plate beneath the Eurasian Plate (Figs. 1, 3A, 3B).

3. Methods

3.1. Elevation differentiation

To compare the elevation differentiation among *Cautleya*, *Roscoea* and their sister taxon, *Hedychium*, we obtained elevation information from the Global Biodiversity Information Facility (http://data.gbif.org/) and our own field collections using GPS. We excluded non-independent overlapping observations from the same location. Eventually, we analyzed 511, 105, and 335 observations of *Hedychium*, *Cautleya*, and *Roscoea*, respectively, in SPSS13 (SPSS, Chicago). Because the distributions of elevation ranges were found to be non-normal for *Hedychium* and *Roscoea*, we performed nonparametric tests (Kruskal–Wallis test) for elevation differentiation (Figs. 1, 2 and Table S1).

3.2. Molecular sampling and genotyping

Roscoea has a disjunct distribution while *Cautleya* has a continuous distribution from the Himalayas (HIM) to the Northern Indochina (NIC) (Fig. 1). In order to maximize the likelihood that we were sampling most of the genetic diversity within each genus, we intensively sampled populations for *Roscoea*, including 15 species from 58 localities, while we adopted a representative sampling approach for *Cautleya*, including both species from 8 localities (Table S2).

The total genomic DNA was extracted following the CTAB protocol (Doyle and Doyle, 1987). Primer pairs of chloroplast DNA (cpDNA) *psb*A-*trn*H (Techaprasan et al., 2006) and *trn*L-F (Taberlet et al., 1991), and nuclear internal transcribed spacer (nrITS) (Sang et al., 1995) were used for Polymerase Chain Reaction (PCR). PCR was performed in a total of 50 μL 1× PCR buffer (50 mM KCl, 10 mM Tris pH 8.0), 2 mM MgCl$_2$, 0.2 μM dNTP, 1 μM primer, 0.25 U Taq DNA polymerase with about 10 ng of genomic DNA template. We used the following

PCR conditions: 94 °C for 5 min, followed by 35 cycles at 94 °C for 30 s, *annealing temperatures* for 30 s at 72 °C for 1.5 min, followed by a final extension period at 72 °C for 15 min. The *annealing temperatures* were 53 °C, 56 °C and 56 °C for *psb*A-*trn*H, *trn*L-F and nrITS respectively. PCR products were purified using polyethylene glycol (PEG800). Then the purified products were bidirectionally sequenced using the PCR primers in the ABI 3730 DNA Analyzer (Applied Biosystems, Foster City, CA). We directly sequenced the nrITS, *psb*A-*trn*H and *trn*L-F regions from ca. 850 *Roscoea* and 14 *Cautleya* individuals. DNA sequences (including nrITS and *trn*K) for the remaining taxa in the genus-level phylogeny were downloaded from GenBank (Table S3). Based on the haplotype network representative nrITS haplotypes of *Roscoea* were selected for the genus-level phylogeny (Figs. 3, 4).

Sequences were aligned using MUSCLE merger (Edgar, 2004) through MAFFT aligner (Katoh et al., 2002) implemented in SATÉ (Liu et al., 2012b), followed by manual adjustments in MEGA5 (Tamura et al., 2011). Allelic phases of nrITS were inferred using PHASE (Stephens et al., 2001; Harrigan et al., 2008). To exclude the impact of recombinations on the concerted evolution of nrITS, we filtered the recombination of nrITS within *Roscoea* using IMGC (Woerner et al., 2007). Haplotypes were inferred in DNASP 5.1 (Librado and Rozas, 2009). Five DNA datasets were used in following analyses: three individual-level datasets, including *Hedychium*, *Cautleya* and *Roscoea*, and two genus-level datasets, including Musaceae, Costaceae and Zingiberaceae (Tables S3, S4).

3.3. Molecular network

Median-Joining networks (Bandelt et al., 1999) of nrITS, fnrITS and cpDNA (*psb*A-*trn*H + *trn*L-F) were constructed using NETWORK 4.6 (http://fluxus-engineering.com) with star contraction under maximum-parsimony execution for nrITS. To visualize the evolutionary origin of *Roscoea* through gene trees, Neighbor-Net networks of haplotypes were constructed using NeighborNet method (Bryant, 2003) based on Neighbor-Joining distances (Saitou and Nei, 1987) in SPLITSTREE4 (Huson and Bryant, 2006).

3.4. Molecular phylogeny

To statistically test phylogenetic compatibility between nrITS and cpDNA of *Roscoea* in individual-level datasets, and nrITS and *trn*K in generic-level datasets (Table S4), we did an incongruence-length difference test (Farris et al., 1994) through PAUP* 4.0b10 (Swofford, 2003). For nrITS and cpDNA of *Roscoea*, to ensure that all variable sites were included and to optimize computation time, we used CD-HIT Suite to minimize the number of homologous sequences (Huang et al., 2010) with the sequence identity threshold set to 1, which means sequences with 100% identity were reduced to a single sequence. Because the number of unique sequences of nrITS (326 sequences) was different from cpDNA (106 sequences), two dataset combinations were used in the compatibility tests. One combination included all of the cpDNA sequences that corresponded to each nrITS sequence, while another combination contained all of the nrITS sequences and their corresponding cpDNA sequences. For nrITS and *trn*K, 103 taxa were used to test phylogenetic compatibility. We run 100 replicates for each data combination, each with 100 heuristic searches. The results suggested that nrITS and cpDNA of *Roscoea* were phylogenetically incompatible ($P = 0.01$) and nrITS and *trn*K were compatible ($P = 0.06$). Thus, nrITS and cpDNA of *Roscoea* were analyzed separately and nrITS and *trn*K were integrated together.

Maximum parsimony (MP) analyses were conducted using the heuristic search in PAUP with 100 random addition sequence replicates and tree bisection-reconnection (TBR) branch swapping. All character states were treated as equally weighted. Bootstrap values were obtained with 1000 bootstrap replicates. In each bootstrap replicate, we performed 100 random addition sequence replicates followed by TBR
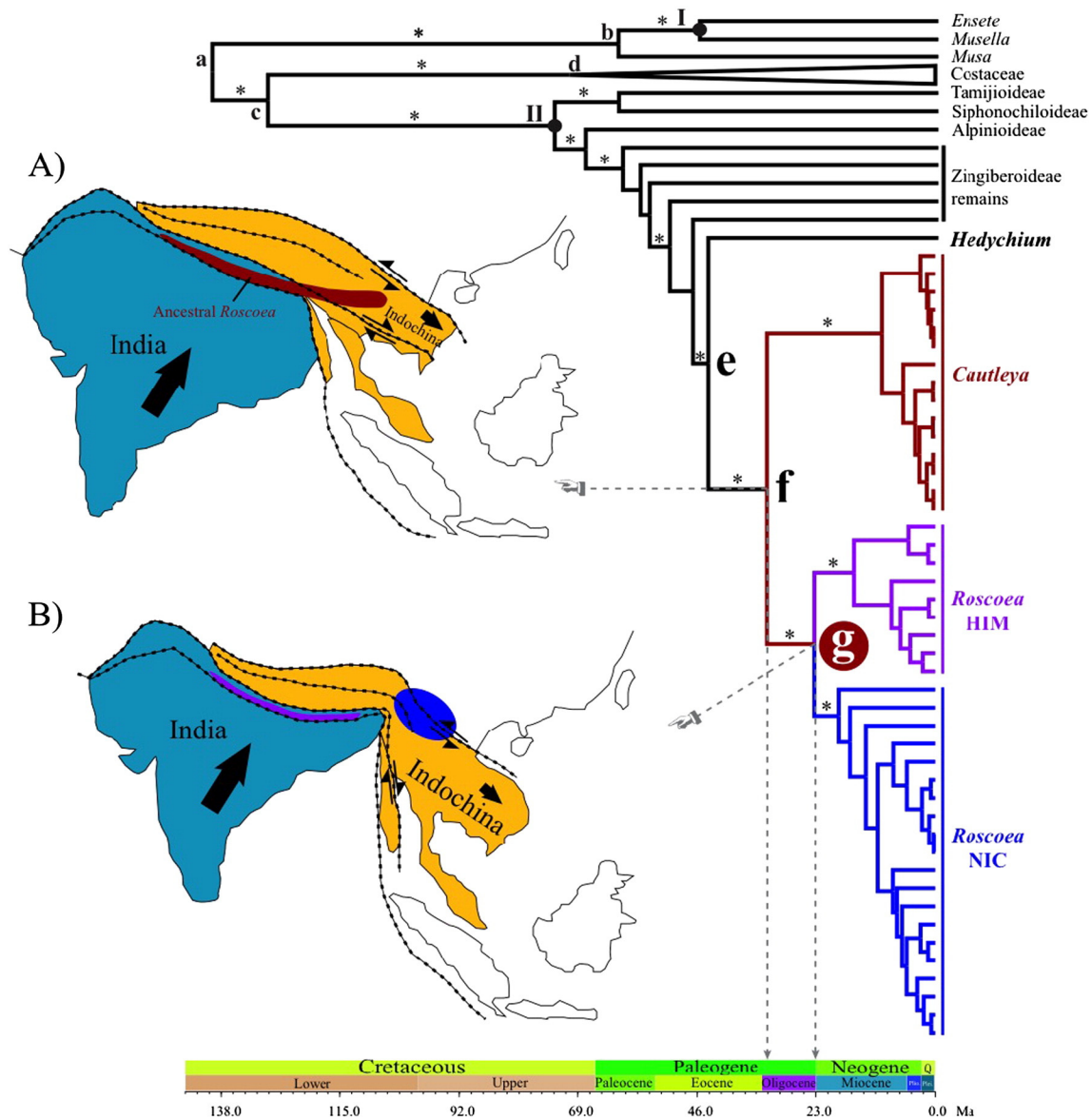
Fig. 3. Evolution of *Cautleya* and *Roscoea* with associated tectonic events. (I) and (II) are fossil calibration nodes. (a–d) are reference nodes compared with previous publications (Table 1). (e) Origination of the common ancestor of *Cautleya* + *Roscoea* at ~44 (29–65) Ma, being related to the first uplift of the Himalayan–Tibetan Plateau. (f and A) *Roscoea* diverged from *Cautleya* at ~32 (18–50) Ma caused by the second stage of uplift. (g and B) Evolutionary split between HIM *Roscoea* and NIC *Roscoea* at ~23 (13–38) Ma probably caused by a rapid lateral extrusion of Indochina with the third uplift. Dashed lines on A and B represent the suture systems show in Fig. 1. "*" indicates stable braches with Bayesian support > 0.90, except node e > 0.80. Brown circle at node (g) indicates *Roscoea* had continuous distribution across the Himalayas before ~23 Ma and then was partitioned by a sudden vicariance event (Fig. S5). Detailed branch information is shown in Fig. S1. Q = Quaternary. Plio. = Pliocene. Plei. = Pleistocene.

swapping, mulTrees on and keeping no more than 1000 trees per random addition sequence replicate.

Bayesian inference (BI) was implemented in MRBAYES 3.1.2 (Ronquist and Huelsenbeck, 2003). The best-fitting nucleotide substitution models for each dataset were selected using the Akaike Information Criterion (AIC), were carried out in jModelTest 0.1 (Posada, 2008). Two independent Bayesian runs were performed through 1,000,000 generations with four Markov chains. A consensus tree was calculated after discarding the first 25% trees as a burn-in period. The best-fitting nucleotide substitution models for each dataset are presented in Table S4.

Maximum likelihood (ML) based inference of phylogenetic trees was executed in RAxML-HPC BlackBox 7.4.4 (Stamatakis, 2006; Stamatakis et al., 2008) on Cyberinfrastructure for Phylogenetic Research (CIPRES) Science Gateway 3.3 (http://www.phylo.org/portal2) (Miller et al., 2010). Bootstrapping was automatically completed when certain criteria were met (BlackBox), instead of specifying the replicates of bootstraps. A best tree was found using ML search.

To avoid long-branch attraction, we only used Zingiberaceae to ascertain the monophyly of subfamilies in MP analysis for nrITS dataset. Phylogenetic trees of BI and ML were also reconstructed for Zingiberaceae. Generally, tree topologies among these three methods (MP, BI, ML) were congruent for each dataset and among datasets (Figs. S1, S2). MP, BI, ML analyses of nrITS and nrITS + *trn*K confirmed the monophylic relationship among subfamilies in Zingiberaceae. Monophyly of *Cautleya*, *Roscoea* and *Hedychium* was also inferred. *Hedychium* and *Larsenianthus* formed a strong monophyly. Because *Larsenianthus* are endemic to northeastern India including only four species and its elevation within the elevation range of *Hedychium* (Kress et al., 2010), *Hedychium* + *Larsenianthus* branches were represented as *Hedychium*.
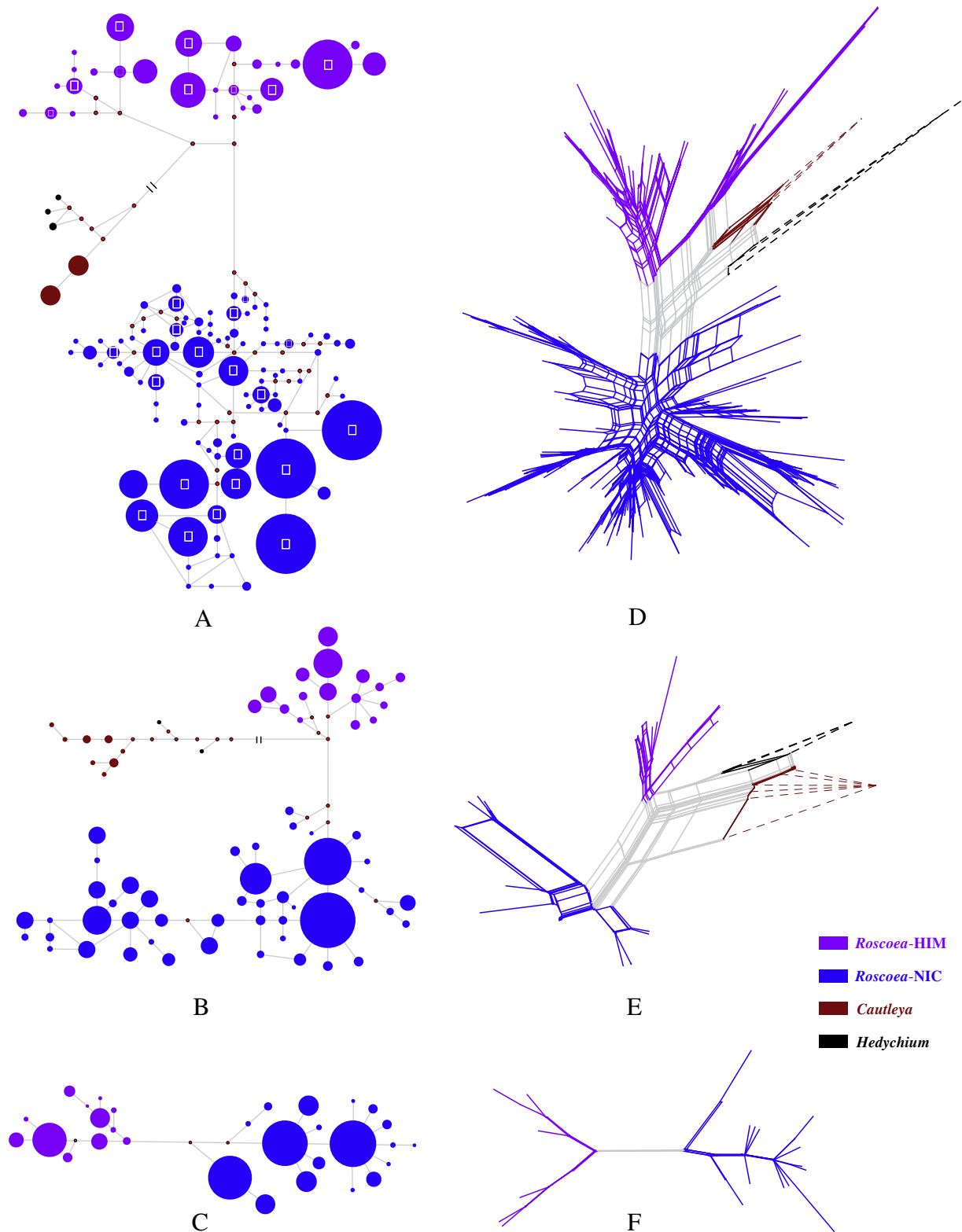
Fig. 4. Haplotype networks of *Roscoea*. (A–C) are estimated from NETWORK and (D–F) are estimated from SPLITSTREE. (A and D) nrITS networks. (A) White dots on the sequence network are the representative types for molecular dating in fossil calibration. (B and E) cpDNA networks. (C and F) Networks of the recombination-filtered nrITS. Haplotype numbers of HIM *Roscoea* versus NIC *Roscoea*, respectively, were 47:124 (nrITS), 12:18 (fnrITS) and 17:45 (cpDNA). (D and E) Dashed lines indicate reduction of topology of *Cautleya* and *Hedychium* derived from Fig. S3.

3.5. Estimation of divergence times

Because the topology of the genus-level nrITS phylogeny was identical to the combined reconstruction of nrITS + *trn*K and the nrITS dataset contained a relatively balanced number of samples for each genus of Zingiberaceae, the nrITS dataset was used to estimate phylogenetic-calibration times through two reliable fossil calibrations (Table 1). No fossil record is available for *Roscoea* and its close relatives. In order to

obtain relatively reliable and reasonable divergence timescales, we used a two-step time indirect estimation, fossil calibration in the distantly related branches and the secondary calibration.

3.5.1. Fossil calibration

The most reliable fossil record of Zingiberales is the seed of *Ensete oregonense* (Musaceae), dated to be 43-million-years old (Manchester and Kress, 1993). This fossil time served as the minimum divergence time between *Ensete* and *Musella* according to their sister relatives (Kress and Specht, 2005; Li et al., 2010; Liu et al., 2010). The splitting time of *Ensete–Musella* should be less than the crown time of Musaceae at the late Cretaceous (Kress and Specht, 2005; Christelová et al., 2011). Thus, in the *lognormal prior* of BEAST, offset was set to 43 Ma, log(mean) was 1.0 and log(stdev) was 0.5.

Another reliable fossil record at the family level includes macrofossils of the Late-Cretaceous *Zingiberopsis* (Hickey and Peterson, 1978). Based on the rolled-leaf hispine beetles' damage on the leaf of *Zingiberopsis*, Wilf et al. (2000) concluded that the adaptive radiations of specialized hispine beetles were associated with the radiation of Zingiberaceae during the late Cretaceous or earlier. Thus, the late Cretaceous (~65 Ma) served as the minimum crown time of Zingiberaceae. Moreover, the radiation of Zingiberaceae should follow than the origination of Zingiberaceae around 105 ± 4 Ma (Kress and Specht, 2005). Therefore, we used *lognormal prior*, which offset was 65 Ma, log(mean) was 2.0 and log(stdev) was 1.0.

3.5.2. Secondary calibration

Hedychium were used as outgroup due to their monophyletic position in relation to *Roscoea* in the fossil calibrated tree (Figs. 3, S1). We used two time points for secondary calibration: the crown time of *Hedychium + Cautleya + Roscoea* and the divergence time between *Roscoea* and *Cautleya*. Estimated times of UERC under fossil calibration were used in secondary calibration based on the Bayes Factor (Table S5). UERC was used in secondary calibration with *lognormal prior*.

3.5.3. BEAST running

Molecular dating of the genus-level phylogeny based on Bayesian MCMC algorithm was performed in BEAST 1.7.4 (Drummond and Rambaut, 2007) on the Cyberinfrastructure for Phylogenetic Research (CIPRES) Science Gateway 3.3 (http://www.phylo.org/portal2) (Miller et al., 2010). Nucleotide substitution models were the same as those used in MrBayes, described above. Tree prior was set to Yule Process Speciation model. Analysis included both uncorrelated lognormal relaxed clock (ULRC) and uncorrelated exponential relaxed clock (UERC), using two independent replicates with length of chain was 40,000,000. Convergences were checked in TRACER 1.5 (http://tree.bio.ed.ac.uk/software/tracer). The best-fitting molecular clock model (ULRC vs. UERC) was selected using Tracer according to the Bayesian

Factor between runs estimated using marginal likelihood (Suchard et al., 2001). Because posterior probabilities of some internal nodes in Zingiberoideae were lower than 0.90, an additional eight independent replicates were run in BEAST to test the stability of objective divergence times among *Cautleya*, *Roscoea* and *Hedychium* using the best-fitting molecular clock model UERC (Table S6). A maximum clade credibility (MCC) tree with median heights was produced using Treeannotator 1.6.2 after burning 25% trees using the result of first run. Trees were visualized using FIGTREE 1.3.1. We also excluded the unstable taxa (indicated in Table S3) in Zingiberoideae to ascertain the targeted divergence time again with two independent runs. The targeted divergence times were stable in twelve runs despite the fact that the position of unstable taxa was variable (Table S6). We found that if the strong monophyly was supported at family/subfamily level, the date of the high-supported-value node would be stable.

3.6. Ancestral area reconstructions

Biogeographic events (vicariance vs. dispersal) and common ancestral area of *Roscoea* were inferred using three methods: (1) statistical dispersal-vicariance analysis (S-DIVA) (Ronquist, 1997; Yu et al., 2010); (2) Bayesian binary MCMC (BBM); (3) a likelihood approach using the dispersal–extinction–cladogenesis model (DEC) (Ree and Smith, 2008). Haplotype datasets of nrITS and cpDNA and trimmed fossil-calibration tree were used to biogeographic reconstructions. All models were implemented in RASP (http://mnh.scu.edu.cn/soft/blog/RASP). We defined three biogeographic areas according to the distribution range of *Roscoea*, *Cautleya* and *Hedychium*: the Himalayas (HIM), the north of Indochina (NIC) and tropical area. *Roscoea* was portioned into HIM and NIC. *Cautleya* contained HIM and NIC. *Hedychium* contained all three areas. 40,000 trees obtained from BEAST analysis were inputted into RASP. 5000 random trees were used for S-DIVA (Ronquist, 1997; Yu et al., 2010) and BBM analysis (http://mnh.scu.edu.cn/soft/blog/RASP). MCC tree produced in BEAST analysis was used as a condense tree. For the BBM analysis, the number of cycles was set to 100,000 with 20 chains. Among-site rate variation was based upon a gamma distribution.

For DEC analysis (Ree and Smith, 2008), we assumed four dispersal parameters. One, dispersal among three areas were free (rate = 1.0) before crown time of *Hedychium + Cautleya + Roscoea*, because we assumed uplift of the Himalayan–Tibetan Plateau was beginning and pantropical elements could easily be distributed to higher elevations (Morley, 2007). Two, dispersal between HIM and NIC was free (rate = 1.0) and dispersal from tropical area to HIM and NIC was reduced (rate = 0.5) before divergence of *Cautleya* and *Roscoea*, because the Himalayan–Tibetan Plateau had reached a certain elevation for the formation of ancestor of *Cautleya* and *Roscoea*. Three, dispersal between HIM and NIC was also free (rate = 1.0) and dispersal from tropical area to HIM and NIC became increasingly reduced (rate =

Table 1
Divergence times based on fossil calibration under uncorrelated exponential relaxed clock (UERC). Nodes are available in Figs. 3 and S1. 95%HPD is 95% highest posterior density. Results of uncorrelated lognormal relaxed clock (ULRC) are appended in Table S7. Ma is million years ago.

Node	Taxa	Fossil calibration	Median (95%HPD) (Ma)	Reference time
I	*Musella–Ensete* divergence	Offset = 43, log(mean) = 1.0, log(sd) = 0.5	45.49 (43.71–48.55)	
II	Zingiberaceae crown	Offset = 65, log(mean) = 2.0, log(sd) = 1.0	73.43 (65.19–105.92)	
a	Root crown		139.68 (99.72–203.44)	107–114 (Kress and Specht, 2005)
b	Musaceae crown		61.16 (47.85–89.88)	50–87 (Kress and Specht, 2005) 57.8–80.5 (Christelová et al., 2011)
c	Zingiberaceae–Costaceae divergence		129.01 (95.88–186.67)	99–109 (Kress and Specht, 2005)
d	Costaceae crown		70.65 (40.18–112.45)	47–74 (Kress and Specht, 2005)
e	*Hedychium + Cautleya + Roscoea* crown		43.88 (28.60–64.72)	
f	*Cautleya–Roscoea* divergence		32.42 (17.87–49.53)	
g	*Roscoea* split		23.28 (13.20–37.80)	

0.1) before split of HIM *Roscoea* and NIC *Roscoea*, because the elevation of the Himalayan–Tibetan Plateau was fit with the origination of *Roscoea* ancestor. And four dispersal between HIM and NIC and dispersal from tropical area to HIM and NIC basically stopped (rate = 0.1 or 0.0) after split of NIC *Roscoea* and NIC *Roscoea*, because the continued increase in elevation and the extrusion of Indochina. Fossil-calibration trees and secondary-calibration trees were use for biogeographic reconstructions.

4. Results

4.1. Elevation differentiation

The genera were found at different mean elevations, from low to high: *Hedychium* (1419 ± 31 m; N = 493), *Cautleya* (2207 ± 52 m; N = 105) and *Roscoea* (2767 ± 33 m; N = 335) (Fig. 2 and Table S1). Both chi-square values of a nonparametric test and *F* values of Homogeneity of Variances Test indicate that elevation differentiation among alpine gingers is significant ($P < 0.001$). The segregation of genera along an elevational range suggested that their divergences may be associated with the uplift of the Himalayan–Tibetan Plateau.

4.2. Sequence characteristics

We tested our hypotheses with five DNA datasets (Tables S2–S4). Three haplotype data sets (nrITS, recombination-filtered nrITS and cpDNA *psb*A-*trn*H + *trn*L-F) obtained from approximately 850 individuals of *Roscoea* in 15 (out of 21) species, 14 individuals in the two species of *Cautleya*, and one individual of each of two species of *Hedychium* were used to examine the evolution of the disjunct species of *Roscoea*. Another two DNA data sets were used to reconstruct a genus-level phylogeny of the family Zingiberaceae: one set included 194 taxa with nrITS sequence data; the other set included 103 taxa with nrITS + *trn*K sequence data. The nrITS data set was used to estimate divergence times of the lineages. DNA fragments sequenced in this study were deposited in GenBank as haplotypes (accessions KF906847–KF907101).

4.3. Network and phylogeny

We did not detect genetic divergence between HIM and NIC *Cautleya* lineages, indicating no significant biogeographic divergence within *Cautleya* between these two regions. However, both haplotype networks and phylogenies strongly demonstrated a deep split between HIM *Roscoea* and NIC *Roscoea*, with no nrITS sequences or cpDNA haplotypes shared between the two areas (Figs. 4, S3, S4). HIM *Roscoea* exhibited simpler nrITS network relationship than NIC *Roscoea*. *Cautleya* is genetically most similar to the outgroup *Hedychium* while HIM *Roscoea* is more similar to *Cautleya* and *Hedychium* than to NIC *Roscoea*. Furthermore, the evolutionary divergence between HIM and NIC species of *Roscoea* is equivalent to the genus-level split between *Roscoea* and *Cautleya*, indicating a burst of diversification in *Roscoea*. The topology of the genus-level phylogenies based on different methods (Bayesian inference, maximum likelihood and maximum parsimony) and different data sets (nrITS and nrITS + *trn*K) were almost identical to the most recent classification of Zingiberaceae (Kress et al., 2002) (Figs. S1, S2).

4.4. Divergence times

Molecular dating estimates by uncorrelated exponential relaxed clock (UERC) were compatible with uncorrelated lognormal relaxed clock (ULRC) under fossil calibration (Tables 1, S7). Moreover, Bayesian factors determined that UERC was better than ULRC (Log10 Bayes factors = 4.69, Table S5). Thus, the following discussion focuses on the results of UERC. Although there were unstable taxa in the fossil

calibration phylogeny, they did not affect the dates of objective nodes (a–g) through the comparison of twelve-runs (Table S6).

Ninety-five percent highest posterior density (95%HPD) ages of key nodes (a–d) were compatible with the ages obtained in previous research (Figs. 3, S1 and Table 1). The crown splitting time of *Hedychium* + *Cautleya* + *Roscoea* was ~44 Ma (median time, 95%HPD: 29–65 Ma). *Roscoea* diverged from *Cautleya* at ~32 Ma (95%HPD: 18–50 Ma). The split between HIM *Roscoea* and NIC *Roscoea* dated to ~23 Ma (95%HPD: 13–38 Ma). The times of secondary split between HIM *Roscoea* and NIC *Roscoea* were ~25 Ma (95%HPD: 17–35 Ma) and ~21 Ma (95%HPD: 13–31 Ma) for nrITS and cpDNA respectively (Table S8), which approximates to the fossil-based estimation that partly excluded the impact of hybridization and sample size of *Roscoea* on time estimation.

4.5. Biogeographic ancestral reconstructions

Using S-DIVA, BBM and DEC revealed that the common ancestral area of *Roscoea* covered HIM and NIC before ~23 Ma (node g, Figs. 3, S1). The proportions of common ancestral areas, estimated by the three datasets (Table S4) were 1.0/1.0/1.0 (S-DIVA), 0.50/0.62/0.61 (BBM) and 1.0/1.0/1.0 (DEC). Only one vicariance event was detected at ~23 Ma in the split of *Roscoea* into two groups (Figs. 3, S5). Because DEC connected geological events to plant migration events using hypothesized parameters, our discussion on biogeographic construction based on this rational result.

5. Discussion

Combining molecular divergence times of biological organisms and geological events on a tectonic scale can construct a more meaningful bridge to understand the correlation between organismic evolution and tectonic events (e.g., Liu et al., 2002; Zhang et al., 2006; Che et al., 2010; Mao et al., 2010, 2012; Yu et al., 2014). Here, we integrate multiple lines of evidence in alpine gingers, such as biological characteristics, phylogenetic inferences and molecular dating, as well as supports from other studies in plants (e.g., Liu et al., 2002; Mao et al., 2010) and animals (e.g., Rüber et al., 2004; Zhang et al., 2006; Che et al., 2010), to test the correlation between evolutionary diversifications of plants and successive occurrence of tectonic events. We also address basic questions about the timing of the early uplift of the Himalayan–Tibetan Plateau and rapid lateral extrusion of Indochina. Although our estimation of diversification timescale in alpine gingers agrees well with previous molecular dating efforts in the ginger family (Table 1), we were still cautious to interpret these molecular dating outputs considering potential effects of error-introducing factors, such as the lack of the direct fossil calibrations and uneven species sampling among lineages.

5.1. Splits among genera reflecting two early uplifts of the Himalayan–Tibetan Plateau

Uplifts of the Himalayan–Tibetan Plateau, caused by crustal thickening, spanned from the beginning of the Eocene (~40–50 Ma) to current times (Harrison et al., 1992; Shi et al., 1998; Yin and Harrison, 2000; Replumaz and Tapponnier, 2003; Aikman et al., 2008; Jain, 2014). The well-supported monophyly of *Cautleya* + *Roscoea* and the clear separation between the two genera in their molecular diversity, elevational distribution, and fundamental life history traits suggested that their diversifications were probably driven by two early uplifts of the Himalayan–Tibetan Plateau. First, the deep divergence between the lower elevation *Hedychium* and the common ancestor of *Cautleya* + *Roscoea* at ~44 (29–65) Ma (Fig. 3, Tables 1, S6) was related to the uplift and associated climate change during the middle Eocene (~40–50 Ma) (Harrison et al., 1992; Raymo and Ruddiman, 1992; Chung et al., 1998; Replumaz and Tapponnier, 2003; Aikman et al., 2008). This age fell in line with a previous investigation on the lineage divergence of

the Asiatic Salamanders which also well correlated the rapid uplift of the Himalayan–Tibetan Plateau during ~40–51 Ma (Zhang et al., 2006).

Subsequently, *Roscoea* diverged from *Cautleya* at ~32 (18–50) Ma, that is synchronous with a second rapid uplift of the Himalayan–Tibetan Plateau at the onset of the Oligocene to the Eocene (~30–40 Ma) (Chung et al., 1998; Replumaz and Tapponnier, 2003). The deep split of lineages in spiny frogs around 27 (19–36) Ma (Che et al., 2010), which was proposed to be triggered by rapid uplift of the Himalayan–Tibetan Plateau, is consistent with our age estimation. Putting together, although previous studies proposed that many biological diversifications were link to early uplifts of the Himalayan–Tibetan Plateau that occurred roughly either during 35–45 Ma or 25–35 Ma (Favre et al., 2014), the early diversifications of high-elevation gingers well reflected uplifts of the plateau during both periods for the first time.

5.2. Disjunct distributions of Roscoea resulting from the lateral extrusion of Indochina

The lateral extrusion of Indochina from the South China Block, including lateral movement southeast of the Tibetan Plateau around the eastern Himalayan syntaxis, was a striking tectonic episode in Asia (Tapponnier et al., 1990; Leloup et al., 2001; Bai et al., 2010; Cao et al., 2011; J. Liu et al., 2012; Xu et al., 2012). Although geological evidences suggested that the Indochina Block sheared along the Ailao Shan-Red River faults (ASRR) can be postdated to ~36 Ma, the most rapid slip of Indochina likely occurred between ~22 Ma and ~25 Ma (Leloup et al., 2001) corresponding to the hard Indo-Eurasian collision (Wang et al., 2006). Meanwhile, rock metamorphism in the eastern Himalayan syntaxis had a peak at 23 Ma (Zhang et al., 2012), large modification of the Yangtze River induced by rapid extrusion of Indochina at the Oligocene/Miocene boundary (~23 Ma) (Zheng et al., 2013) and the disconnection of the Yarlung Tsangpo-Irrawaddy river in the Early Miocene (~20 Ma) driven by rapid deformation of the eastern Himalayan syntaxis (Robinson et al., 2014), indicating that the Asian lithosphere experienced a huge alteration around the Oligocene/Miocene boundary. It remains debated about the relative importance of crustal thickening (plateau uplifts) versus lateral extrusion contributed to the Indo-Asia collision (Tapponnier et al., 2001; Yang and Liu, 2009). However, the lateral extrusion of Indochina is likely correlated with an early uplift of the Himalayan–Tibetan Plateau (Shi et al., 1998) and the further geological evidence did suggest the extensive uplift during the Oligocene/Miocene boundary (Guo et al., 2002).

Phylogenetic and molecular dating analyses of *Roscoea* suggested that the HIM and NIC species, with a ~500 km wide gap separating the disjunct areas, are reciprocally monophyletic. Ancestral area reconstructions indicated that *Roscoea* originated in the Himalayan region and then expanded its ranges to occupy both HIM to NIC. The extensive population-level sampling of most species of *Roscoea* from two regions revealed that no haplotype was shared between them. Such allopatric divergence was most likely caused by a single relatively rapid vicariant event (Figs. 3, S5). Molecular dating revealed that HIM and NIC *Roscoea* species split into distinct lineages at ~23 (13–38) Ma (Fig. 3 and Tables 1, S6), which is likely correlated with the approximate geological time of the remarkable lateral shear of ASRR when Indochina was displaced >500 km southeastwards of South China by the Indo-Eurasian collision (Tapponnier et al., 1990; Lacassin et al., 1997). In fact, this vicariant divergence in some animals was suggested to result from the synchronous uplift of the Himalaya–Tibetan Plateau with lateral extrusion of Indochina (Che et al., 2010). A few animal and plant groups in the high-altitude region were dated to have originated or diverged from their sister group around the Oligocene/Miocene boundary, supporting that this lateral extrusion of Indochina probably occurred synchronously with the extensive plateau uplift (Liu et al., 2002; Rüber et al., 2004; Zhang et al., 2006; Mao et al., 2010). Overall, these biogeographic results seem together to support the tectonic hypothesis that around the Oligocene/Miocene boundary the rapid

lateral extrusion of Indochina occurred synchronously with extensive uplift of the Himalayan–Tibetan Plateau after the Indo-Eurasian collision.

6. Conclusions

The Indo-Eurasian collision caused a series of large-scale orogenic events. Our findings based on an integrative methodology in plants provide an independent line of evidence for interpreting these geological events. Two early uplifts of the Himalayan–Tibetan Plateau and the third with a rapid lateral extrusion of the Indochina Block most likely shaped the early biogeographic history of two alpine ginger genera *Cautleya* and *Roscoea*. We predict that other plants of this region, which possess similar distribution ranges from the Himalayas to the north of Indochina, will show similar biogeographic history as illustrated here. Our results also indicate that herbaceous species with the reduced ability for long-distance seed dispersal and restricted pollen flow may harbor unique genetic imprints that reflect ancient geological and environmental changes in this region.

Appendix A. Supplementary data

Supplementary data to this article can be found online at http://dx.doi.org/10.1016/j.gr.2015.02.004.

References

Aikman, A.B., Harrison, T.M., Lin, D., 2008. Evidence for early (>44 Ma) Himalayan crustal thickening, Tethyan Himalaya, southeastern Tibet. Earth and Planetary Science Letters 274, 14–23.

An, Z., Kutzbach, J., Prell, W., Porter, S., 2001. Evolution of Asian monsoons and phased uplift of the Himalaya–Tibetan Plateau since Late Miocene time. Nature 411, 62–66.

Auvray, G., Newman, M.F., 2010. A revision of *Cautleya* (Zingiberaceae). Edinburgh Journal of Botany 67, 451–465.

Bai, D., Unsworth, M.J., Meju, M.A., Ma, X., Teng, J., Kong, X., Sun, Y., Sun, J., Wang, L., Jiang, C., Zhao, C., Xiao, P., Liu, M., 2010. Crustal deformation of the eastern Tibetan plateau revealed by magnetotelluric imaging. Nature Geoscience 3, 358–362.

Bandelt, H.J., Forster, P., Röhl, A., 1999. Median-joining networks for inferring intraspecific phylogenies. Molecular Biology and Evolution 16, 37–48.

Bryant, D., 2003. Neighbor-net: an agglomerative method for the construction of phylogenetic networks. Molecular Biology and Evolution 21, 255–265.

Cao, S., Liu, J., Leiss, B., Neubauer, F., Genser, J., Zhao, C., 2011. Oligo-Miocene shearing along the Ailao Shan–Red River shear zone: constraints from structural analysis and zircon U/Pb geochronology of magmatic rocks in the Diancang Shan massif, SE Tibet, China. Gondwana Research 19, 975–993.

Chatterjee, S., Goswami, A., Scotese, C.R., 2013. The longest voyage: tectonic, magmatic, and paleoclimatic evolution of the Indian plate during its northward flight from Gondwana to Asia. Gondwana Research 23, 238–267.

Che, J., Zhou, W.W., Hu, J.S., Yan, F., Papenfuss, T.J., Wake, D.B., Zhang, Y.P., 2010. Spiny frogs (Paini) illuminate the history of the Himalayan region and Southeast Asia. Proceedings of the National Academy of Sciences of the United States of America 107, 13765–13770.

Christelová, P., Valárik, M., Hřibová, E., De Langhe, E., Doležel, J., 2011. A multi gene sequence-based phylogeny of the Musaceae (banana) family. BMC Evolutionary Biology 11, 103.

Chung, S.-L., Lo, C.-H., Lee, T.-Y., Zhang, Y., Xie, Y., Li, X., Wang, K.-L., Wang, P.-L., 1998. Diachronous uplift of the Tibetan plateau starting 40 Myr ago. Nature 194, 769–773.

Cowley, E.J., 2007. The Genus *Roscoea*. The Royal Botanic Gardens, Kew.

Doyle, J.J., Doyle, J.L., 1987. A rapid DNA isolation procedure for small quantities of fresh leaf tissue. Phytochemical Bulletin 19, 11–15.

Drummond, A.J., Rambaut, A., 2007. BEAST: Bayesian evolutionary analysis by sampling trees. BMC Evolutionary Biology 7, 214.

Edgar, R.C., 2004. MUSCLE: multiple sequence alignment with high accuracy and high throughput. Nucleic Acids Research 32, 1792–1797.

Fan, Y.-L., Li, Q.-J., 2012. Stigmatic fluid aids self-pollination in *Roscoea debilis* (Zingiberaceae): a new delayed selfing mechanism. Annals of Botany 110, 969–975.

Farris, J.S., Källersjö, M., Kluge, A.G., Bult, C., 1994. Testing significance of incongruence. Cladistics 10, 315–319.

Favre, A., Packert, M., Pauls, S.U., Jähnig, S.C., Uhl, D., Michalak, I., Muellner-Riehl, A.N., 2014. The role of the uplift of the Qinghai–Tibetan Plateau for the evolution of Tibetan biotas. Biological Reviews http://dx.doi.org/10.1111/brv.12107.

Guo, Z.T., Ruddiman, W.F., Hao, Q.Z., Wu, H.B., Qiao, Y.S., Zhu, R.X., Peng, S.Z., Wei, J.J., Yuan, B.Y., Liu, T.S., 2002. Onset of Asian desertification by 22 Myr ago inferred from loess deposits in China. Nature 416, 159–163.

Harrigan, R.J., Mazza, M.E., Sorenson, M.D., 2008. Computation vs. cloning: evaluation of two methods for haplotype determination. Molecular Ecology Resources 8, 1239–1248.

Harrison, T.M., Copeland, P., Kidd, W., Yin, A., 1992. Raising Tibet. Science 255, 1663–1670.

Hickey, L.J., Peterson, R.K., 1978. *Zingiberopsis*, a fossil genus of the ginger family from Late Cretaceous to early Eocene sediments of Western Interior North America. Canadian Journal of Botany 56, 1136–1152.

Huang, Y., Niu, B., Gao, Y., Fu, L., Li, W., 2010. CD-HIT Suite: a web server for clustering and comparing biological sequences. Bioinformatics 26, 680–682.

Huson, D.H., Bryant, D., 2006. Application of phylogenetic networks in evolutionary studies. Molecular Biology and Evolution 23, 254–267.

Jain, A.K., 2014. When did India–Asia collide and make the Himalaya? Current Science 106, 254–266.

Katoh, K., Misawa, K., Kuma, K.-i., Miyata, T.,, 2002. MAFFT: a novel method for rapid multiple sequence alignment based on fast Fourier transform. Nucleic Acids Research 30, 3059–3066.

Kress, W.J., Specht, C.D., 2005. The evolutionary and biogeographic origin and diversification of the tropical monocot order Zingiberales. Aliso 22, 619–630.

Kress, W.J., Prince, L.M., Williams, K.J., 2002. The phylogeny and a new classification of the gingers (Zingiberaceae): evidence from molecular data. American Journal of Botany 89, 1682–1696.

Kress, W.J., Mood, J., Sabu, M., Prince, L., Dey, S., Sanoj, E., 2010. *Larsenianthus*, a new Asian genus of gingers (Zingiberaceae) with four species. PhytoKeys 1, 15–32.

Lacassin, R., Maluski, H., Leloup, H., Tapponnier, P., Hinthong, C., iribhakdi, K.S., Chuaviroj, S., Charoenravat, A.,, 1997. Tertiary diachronic extrusion and deformation of western Indochina: structural and ⁴⁰Ar/³⁹Ar evidence from NW Thailand. Journal of Geophysical Research, Solid Earth 102, 10013–10037.

Leloup, P.H., Arnaud, N., Lacassin, R., Kienast, J.R., Harrison, T.M., Trong, T.T.P., Replumaz, A., Tapponnier, P., 2001. New constraints on the structure, thermochronology, and timing of the Ailao Shan-Red River shear zone, SE Asia. Journal of Geophysical Research 106, 6683.

Li, L.-F., Häkkinen, M., Yuan, Y.-M., Hao, G., Ge, X.-J., 2010. Molecular phylogeny and systematics of the banana family (Musaceae) inferred from multiple nuclear and chloroplast DNA fragments, with a special reference to the genus *Musa*. Molecular Phylogenetics and Evolution 57, 1–10.

Librado, P., Rozas, J., 2009. DnaSP v5: a software for comprehensive analysis of DNA polymorphism data. Bioinformatics 25, 1451–1452.

Liu, J.-Q., Gao, T.-G., Chen, Z.-D., Lu, A.-M., 2002. Molecular phylogeny and biogeography of the Qinghai–Tibet Plateau endemic *Nannoglottis* (Asteraceae). Molecular Phylogenetics and Evolution 23, 307–325.

Liu, J.-Q., Wang, Y.-J., Wang, A.-L., Hideaki, O., Abbott, R.J., 2006. Radiation and diversification within the *Ligularia–Cremanthodium–Parasenecio* complex (Asteraceae) triggered by uplift of the Qinghai–Tibetan Plateau. Molecular Phylogenetics and Evolution 38, 31–49.

Liu, A.-Z., Kress, W.J., Li, D.-Z., 2010. Phylogenetic analyses of the banana family (Musaceae) based on nuclear ribosomal (ITS) and chloroplast (*trn*L-F) evidence. Taxon 59, 20–29.

Liu, J., Tang, Y., Tran, M.-D., Cao, S., Zhao, L., Zhang, Z., Zhao, Z., Chen, W., 2012a. The nature of the Ailao Shan–Red River (ASRR) shear zone: constraints from structural, micro-structural and fabric analyses of metamorphic rocks from the Diancang Shan, Ailao Shan and Day Nui Con Voi massifs. Journal of Asian Earth Sciences 47, 231–251.

Liu, K., Warnow, T.J., Holder, M.T., Nelesen, S.M., Yu, J., Stamatakis, A.P., Linder, C.R., 2012b. SATe-II: very fast and accurate simultaneous estimation of multiple sequence alignments and phylogenetic trees. Systematic Biology 61, 90–106.

Liu, J.-Q., Duan, Y.-W., Hao, G., Ge, X.-J., Sun, H., 2014. Evolutionary history and underlying adaptation of alpine plants on the Qinghai–Tibet Plateau. Journal of Systematics and Evolution 52, 241–249.

Manchester, S.R., Kress, W.J., 1993. Fossil *bananas* (Musaceae) *Ensete oregonense* sp. nov. from the Eocene of western North America and its phytogeographic significance. American Journal of Botany 80, 1264–1272.

Mao, K., Hao, G., Liu, J., Adams, R., Milne, R., 2010. Diversification and biogeography of *Juniperus* (Cupressaceae): variable diversification rates and multiple intercontinental dispersals. New Phytologist 188, 254–272.

Mao, K., Milne, R.I., Zhang, L., Peng, Y., Liu, J., Thomas, P., Mill, R.R., Renner, S., S.,, 2012. Distribution of living Cupressaceae reflects the breakup of Pangea. Proceedings of the National Academy of Sciences of the United States of America 109, 7793–7798.

Miller, M.A., Pfeiffer, W., Schwartz, T., 2010. Creating the CIPRES Science Gateway for inference of large phylogenetic trees. Proceedings of the Gateway Computing Environments Workshop (GCE), 14 Nov. 2010, New Orleans, LA, pp. 1–8.

Morley, R.J., 2007. Cretaceous and Tertiary climate change and the past distribution of megathermal rainforests. In: Bush, M.B., Flenley, J.R. (Eds.), Tropical Rainforest Response to Climate Change. Springer Berlin Heidelberg, New York, pp. 1–31.

Ngamriabsakul, C., Newman, M.F., Cronk, Q.C.B., 2000. Phylogeny and disjunction in *Roscoea* (Zingiberaceae). Edinburgh Journal of Botany 57, 39–61.

Posada, D., 2008. jModelTest: phylogenetic model averaging. Molecular Biology and Evolution 25, 1253–1256.

Raymo, M.E., Ruddiman, W.F., 1992. Tectonic forcing of late Cenozoic climate. Nature 359, 117–122.

Ree, R.H., Smith, S.A., 2008. Maximum likelihood inference of geographic range evolution by dispersal, local extinction, and cladogenesis. Systematic Biology 57, 4–14.

Replumaz, A., Tapponnier, P., 2003. Reconstruction of the deformed collision zone between India and Asia by backward motion of lithospheric blocks. Journal of Geophysical Research 108, 2285.

Robinson, R.A.J., Brezina, C.A., Parrish, R.R., Horstwood, M.S.A., Nay Win, O., Bird, M.I., Myint, T., Walters, A.S., Oliver, G.J.H., Khin, Z., 2014. Large rivers and orogens: the evolution of the Yarlung Tsangpo–Irrawaddy system and the eastern Himalayan syntaxis. Gondwana Research 26, 112–121.

Ronquist, F., 1997. Dispersal-vicariance analysis: a new approach to the quantification of historical biogeography. Systematic Biology 46, 195–203.

Ronquist, F., Huelsenbeck, J.P., 2003. MrBayes 3: Bayesian phylogenetic inference under mixed models. Bioinformatics 19, 1572–1574.

Rüber, L., Britz, R., Kullander, S.O., Zardoya, R., 2004. Evolutionary and biogeographic patterns of the Badidae (Teleostei: Perciformes) inferred from mitochondrial and nuclear DNA sequence data. Molecular Phylogenetics and Evolution 32, 1010–1022.

Saitou, N., Nei, M., 1987. The neighbor-joining method: a new method for reconstructing phylogenetic trees. Molecular Biology and Evolution 4, 406–425.

Sang, T., Crawford, D.J., Stuessy, T.F., 1995. Documentation of reticulate evolution in peonies (*Paeonia*) using internal transcribed spacer sequences of nuclear ribosomal DNA: implications for biogeography and concerted evolution. Proceedings of the National Academy of Sciences of the United States of America 92, 6813–6817.

Shi, Y.F., Li, J., Li, B.Y., 1998. Uplift and Environmental Changes of Qinghai–Tibet Plateau in the Late Cenozoic. Guangdong Science and Technology Press, Guangzhou.

Spicer, R.A., Harris, N.B.W., Widdowson, M., Herman, A.B., Guo, S., Valdes, P.J., Wolfe, J.A., Kelley, S.P., 2003. Constant elevation of southern Tibet over the past 15 million years. Nature 421, 622–624.

Stamatakis, A., 2006. Likelihood-based phylogenetic analyses with thousands of taxa and mixed models. Bioinformatics 22, 2688–2690.

Stamatakis, A., Hoover, P., Rougemont, J., 2008. A rapid bootstrap algorithm for the RAxML web servers. Systematic Biology 57, 758–771.

Stephens, M., Smith, N.J., Donnelly, P., 2001. A new statistical method for haplotype reconstruction from population data. The American Journal of Human Genetics 68, 978–989.

Suchard, M.A., Weiss, R.E., Sinsheimer, J.S., 2001. Bayesian selection of continuous-time Markov chain evolutionary models. Molecular Biology and Evolution 18, 1001–1013.

Swofford, D.L., 2003. PAUP*: Phylogenetic Analysis Using Parsimony (*and other methods), Version 4.0b10. Sinauer, Sunderland, Massachusetts, USA.

Taberlet, P., Gielly, L., Pautou, G., Bouvet, J., 1991. Universal primers for amplification of three non-coding regions of chloroplast DNA. Plant Molecular Biology 17, 1105–1109.

Tamura, K., Peterson, D., Peterson, N., Stecher, G., Nei, M., Kumar, S., 2011. MEGA5: molecular evolutionary genetics analysis using maximum likelihood, evolutionary distance, and maximum parsimony methods. Molecular Biology and Evolution 28, 2731–2739.

Tapponnier, P., Lacassin, R., Leloup, P.H., Schärer, U., Dalai, Zhong, Haiwei, Wu, Xiaohan, Liu, Shaocheng, Ji, Lianshang, Z., Jiayou, Z., 1990. The Ailao Shan/Red River metamorphic belt: tertiary left-lateral shear between Indochina and South China. Nature 343, 431–437.

Tapponnier, P., Xu, Z., Roger, F., Meyer, B., Arnaud, N., Wittlinger, G., Yang, J., 2001. Oblique stepwise rise and growth of the Tibet Plateau. Science 294, 1671–1677.

Techaprasan, J., Ngamriabsakul, C., Klinbunga, S., Chusacultanachai, S., Jenjittikul, T., 2006. Genetic variation and species identification of Thai *Boesenbergia* (Zingiberaceae) analyzed by chloroplast DNA polymorphism. Journal Of Biochemistry and Molecular Biology 39, 361–370.

Wang, Y., Fan, W., Zhang, Y., Peng, T., Chen, X., Xu, Y., 2006. Kinematics and ⁴⁰Ar/³⁹Ar geochronology of the Gaoligong and Chongshan shear systems, western Yunnan, China: implications for early Oligocene tectonic extrusion of SE Asia. Tectonophysics 418, 235–254.

Wang, Y.-J., Susanna, A., Raab-Straube, E.V., Milne, R., Liu, J.-Q., 2009. Island-like radiation of *Saussurea* (Asteraceae: Cardueae) triggered by uplifts of the Qinghai–Tibetan Plateau. Biological Journal of the Linnean Society 97, 893–903.

Wilf, P., Labandeira, C.C., Kress, W.J., Staines, C.L., Windsor, D.M., AUen, A.L., Johnson, K.R., 2000. Timing the radiations of leaf-beetles: hispines on gingers from latest Cretaceous to recent. Science 289, 291–294.

Woerner, A.E., Cox, M.P., Hammer, M.F., 2007. Recombination-filtered genomic datasets by information maximization. Bioinformatics 23, 1851–1853.

Wu, T., 1994. Phytogeography of the Zingiberaceae. Journal of Tropical and Subtropical Botany 2, 1–14.

Xu, Z., Ji, S., Cai, Z., Zeng, L., Geng, Q., Cao, H., 2012. Kinematics and dynamics of the Namche Barwa Syntaxis, Eastern Himalaya: constraints from deformation, fabrics and geochronology. Gondwana Research 21, 19–36.

Yang, Y., Liu, M., 2009. Crustal thickening and lateral extrusion during the Indo-Asian collision: a 3D viscous flow model. Tectonophysics 465, 128–135.

Yin, A., 2006. Cenozoic tectonic evolution of the Himalayan orogen as constrained by along-strike variation of structural geometry, exhumation history, and foreland sedimentation. Earth-Science Reviews 76, 1–131.

Yin, A., 2010. Cenozoic tectonic evolution of Asia: a preliminary synthesis. Tectonophysics 488, 293–325.

Yin, A., Harrison, T.M., 2000. Geologic evolution of the Himalayan–Tibetan orogen. Annual Review of Earth and Planetary Sciences 28, 211–280.

Yu, Y., Harris, A.J., He, X., 2010. S-DIVA (Statistical Dispersal-Vicariance Analysis): a tool for inferring biogeographic histories. Molecular Phylogenetics and Evolution 56, 848–850.

Yu, X.Q., Maki, M., Drew, B.T., Paton, A.J., Li, H.W., Zhao, J.L., Conran, J.G., Li, J., 2014. Phylogeny and historical biogeography of *Isodon* (Lamiaceae): rapid radiation in south-west China and Miocene overland dispersal into Africa. Molecular Phylogenetics and Evolution 77, 183–194.

Zhang, Z.Q., Li, Q.J., 2008. Autonomous selfing provides reproductive assurance in an alpine ginger *Roscoea schneideriana* (Zingiberaceae). Annals of Botany 102, 531–538.

Zhang, P., Chen, Y.-Q., Zhou, H., Liu, Y.-F., Wang, X.-L., Papenfuss, T.J., Wake, D.B., Qu, L.-H., 2006. Phylogeny, evolution, and biogeography of Asiatic Salamanders (Hynobiidae). Proceedings of the National Academy of Sciences of the United States of America 103, 7360–7365.

Zhang, Z., Dong, X., Santosh, M., Liu, F., Wang, W., Yiu, F., He, Z., Shen, K., 2012. Petrology and geochronology of the Namche Barwa Complex in the eastern Himalayan syntaxis, Tibet: constraints on the origin and evolution of the north-eastern margin of the Indian Craton. Gondwana Research 21, 123–137.

Zheng, H., Clift, P.D., Wang, P., Tada, R., Jia, J., He, M., Jourdan, F., 2013. Pre-Miocene birth of the Yangtze River. Proceedings of the National Academy of Sciences of the United States of America 110, 7556–7561.